

## Development of uniaxial stress, dilatometry, and microstructuring methods

Clifford Hicks<sup>#</sup>, Elena Hassinger, Markus König, Robert Küchler, Philip Moll, Maja Bachmann, Mark Barber, Jack Bartlett, Toni Helm, Fabian Jerzembeck, You-Sheng Li, Andy Mackenzie, Philippa McGuinness, Nabhanila Nandi, Hilary Noad, Kimberley Putkonen, Kent Shirer, Alexander Steppke, Po-Ya Yang, Elina Zhakina, Tino Zimmerling

Within the PQM department we are pursuing three major areas of technique development. One is uniaxial stress. Uniaxial stress can directly alter the point-group symmetry of crystal lattices, and so typically gives qualitatively different results from hydrostatic pressure. Before 2013 it was a relatively seldom-used method, however through development of piezoelectric-driven stress cells and appropriate sample preparation, the PQM department has greatly expanded the precision and accessible pressure range. A second, complementary area is precision dilatometry, where the ability to resolve fractional length changes  $\Delta L/L$  below  $10^{-8}$  has made dilatometry a useful probe of low-temperature phenomena. The third area is the development of novel microstructuring protocols for quantum materials, using focused gallium and xenon ion beams.

**1. Uniaxial stress: Background and first-generation cells.** We start with two examples of how uniaxial stress is a qualitatively different probe from hydrostatic pressure. The first is  $\text{Sr}_2\text{RuO}_4$ , a metal with moderately heavy charge carriers and unconventional superconductivity below  $T_c = 1.5$  K. Under hydrostatic pressure bandwidths increase, effects of electronic correlation are weakened, and  $T_c$  falls. However the effect of uniaxial stress is completely different. One of the Fermi surfaces of  $\text{Sr}_2\text{RuO}_4$  is nearly circular and passes very close to the Brillouin zone boundary, and

this Fermi surface distorts elliptically, eventually touching the zone boundary. As it does so, a Van Hove singularity in the density of states is tuned to the Fermi level, and one obtains a metal that has both stationary charge carriers, as in an insulator, and fast, conventional quasi-particles. One consequence is a strong enhancement of the superconductivity, including a twenty-fold enhancement in the upper critical field [1].

The case of  $\text{YBa}_2\text{Cu}_3\text{O}_{6+x}$  is opposite: hydrostatic pressure often increases  $T_c$  by strengthening the interactions between atomic sites, however in contrast to  $\text{Sr}_2\text{RuO}_4$  it is arguably more informative not to try to further strengthen superconductivity in the cuprates but rather to weaken it, and reveal alternative ground states. These provide information on the interactions present in the system, including those that may drive the superconductivity. Working with collaborators from MPI-FKF (Stuttgart), we have found that compressing  $\text{YBa}_2\text{Cu}_3\text{O}_{6+x}$  along its  $a$  axis by  $\sim 1\%$  induces long-range charge density wave order [2].

In Fig. 1 we illustrate a first-generation uniaxial stress cell similar to those used for the above-mentioned experiments. The key aspect enabling low-temperature operation is a symmetric arrangement of “tension” and “compression” piezoelectric actuators. These are identical actuators arranged so that their action on sample is opposite, which means that the effect of the actuators’ own thermal contraction as the apparatus is cooled is canceled. Force, either compressive or tensile, is then applied to the sample by applying a voltage differential between the compression and tension actuators.

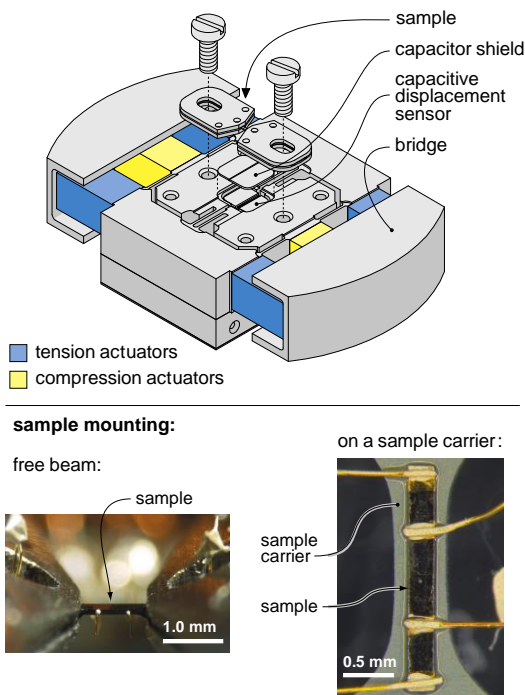


Fig.-1: Top: schematic of a first-generation piezoelectric uniaxial stress cell. The cell incorporates a capacitive displacement sensor. Bottom: two methods to mount samples.

Samples are mounted in this cell in two possible ways. Mechanically robust materials, such as  $\text{Sr}_2\text{RuO}_4$ , may be mounted as free beams, as shown in the lower left of the figure. Force is then applied along the length of this beam. More delicate samples may be affixed to a carrier, as shown in the lower right of the figure, which is then bolted to the cell. Force is applied along the length of the carrier, and the resulting strain is transferred to the sample through the glue layer. In this way we have compressed FeSe, a van der Waals-bonded material, by up to 0,7 %. This is sufficient to drive, in FeSe, a strong polarisation of its nematic susceptibility.

Stress cells based on our designs and licensed through Max Planck Innovation form the commercial basis of a start-up company, Razorbill Instruments [3]. They entered the market in October 2015 and have sold, as of May 2018, 65 pressure cells.

## 2. Advanced uniaxial stress cells.

We are extending development in three directions: (i) larger samples, (ii) better control, and (iii) smaller samples.

- (i) *Larger samples.* Neutron scattering and muon spin rotation experiments typically require relatively large samples. Correspondingly, larger forces are required to achieve a given

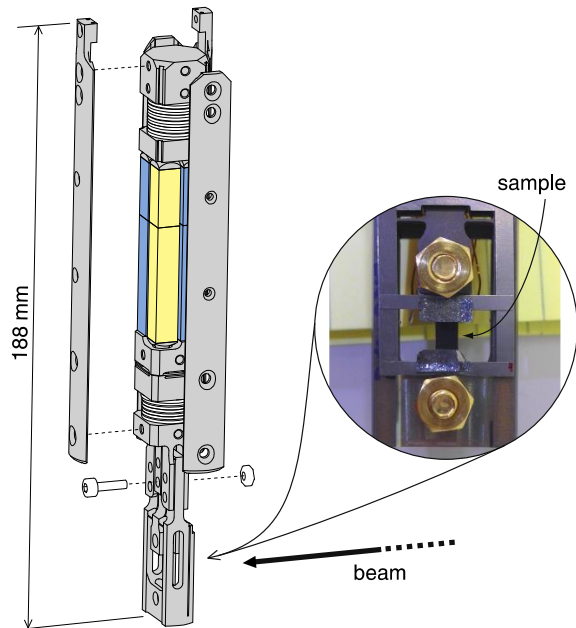


Fig.-2: A piezoelectric uniaxial stress cell suitable for muon spin rotation and neutron scattering experiments. The blue- and yellow-coloured actuators are, as in Fig. 1, the tension and compression actuators.

uniaxial stress. Working with partners at the Technical University of Dresden and the Paul Scherrer Institute, we have built and demonstrated the prototype cell illustrated in Fig. 2. Development of this cell is motivated especially by  $\text{Sr}_2\text{RuO}_4$ : the depolarisation rate of muons implanted into  $\text{Sr}_2\text{RuO}_4$  increases anomalously below  $T_c$ . This response is generally interpreted to indicate a time-reversal symmetry-breaking (TRSB) order parameter, which is very unusual, however the mechanism by which this inference can be made is not known, so doubts still exist.

Because uniaxial stress strongly, and continuously, alters the superconductivity of  $\text{Sr}_2\text{RuO}_4$ , we expect to learn about both the superconductivity of  $\text{Sr}_2\text{RuO}_4$  and the muon technique itself.

- (ii) *Better control.* In the first-generation cells the sensor used to determine the sample strain is a displacement sensor placed in parallel with the sample. This is not ideal because it does not distinguish between an actual change in the sample strain and deformation of the epoxy that holds the sample. We have therefore developed the cell illustrated in Fig. 3, which contains both the displacement sensor and a sensor in series with the sample, that acts as a force sensor. An anomalous increase in applied displacement to achieve a specified force indicates that the sample or epoxy is starting to crack. Using this cell, a uniaxial stress of almost 2 GPa was applied to a sample of  $\text{Sr}_2\text{RuO}_4$ .

- (iii) *Smaller samples.* Most materials can in principle withstand tensile strains of a few percent. However in reality stress concentrates around surface defects, and under tension most samples break at stresses well below their intrinsic strength. Therefore although our stress cells can generally apply both compressive and tensile forces, we are usually compelled to stay on the compression side. This is a meaningful limitation because a number of strain-induced phenomena, such as the sharp increase in  $T_c$  of  $\text{Sr}_2\text{RuO}_4$ , should also occur under tension. Therefore our third major area of development is to reduce the sample size to something that can be shaped and polished with a focused ion beam, in order to obtain higher-quality surfaces.

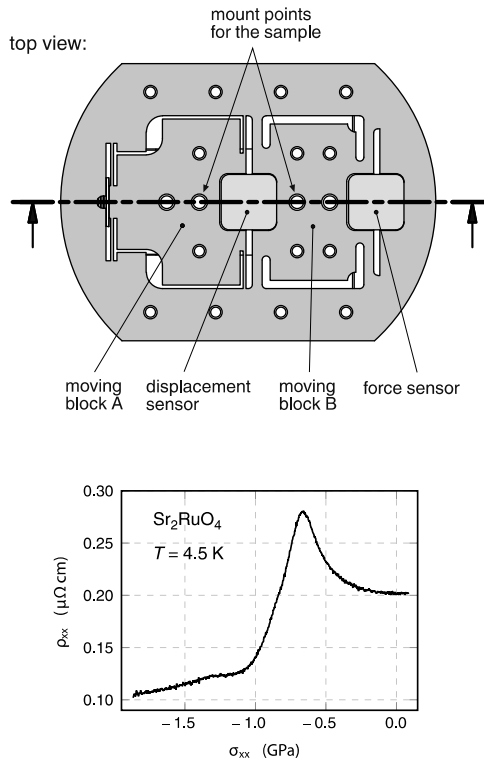


Fig.-3: Top: top view of a pressure cell with combined force and displacement sensors. Piezoelectric actuators drive motion of moving block A, applying a force on the sample that is transferred to moving block B. The force sensor is a capacitive sensor that measures the displacement of block B under this applied force. Bottom: using this cell, a record uniaxial stress of 1.9 GPa was applied to  $\text{Sr}_2\text{RuO}_4$ .

### 3. Dilatometry

Another area of instrument development within the PQM department is high-precision dilatometry. Parallel-plate capacitive dilatometers are a well-established measurement tool, but we have introduced practical advances that enable higher levels of precision [4]. The most substantial was, in 2012, to

simplify and miniaturise the main body of the cell by manufacturing it from a single piece of beryllium copper; this design has been patented and commercialised [5]. The optimised design allows the plates of the capacitive sensor to be almost as wide as the body of the cell itself, which, along with careful fabrication, allows an unprecedented length resolution of  $\delta L = 0.02 \text{ \AA}$  from a cell that fits into a 25 mm diameter. A rendering of this cell is shown in Fig. 4(a).

Since then, further modifications have been introduced. In Fig. 4(b) we illustrate an ultracompact dilatometer, of dimensions  $14 \times 15 \times 16 \text{ mm}$ , that maintains a length resolution of  $0.01 \text{ \AA}$ . This cell fits into the bore of high-field magnets, enabling, for example, a thermodynamic study of field-induced phases in graphite [6].

Another modification is to apply large forces to the sample. In conventional dilatometry the sample is lightly clamped between two plates, and one usually aims to keep this applied force low. However strong uniaxial stress, as we have described above, can drive interesting changes in the properties of many materials. In our dilatometers the moving capacitor plate is guided by leaf springs, and through an increase in the thickness of these leaf springs from 0.25 to 0.70 mm the cell illustrated in Fig. 4(c) can apply forces of up to  $\sim 75 \text{ N}$ . This dilatometer has been applied so far to the study of a magnetic-shape-memory Heusler compound [7], and frustrated magnets [8].

### 4. Microstructuring

Over the past few years facilities dedicated to microstructuring of materials have been set up in our department. The key pieces of equipment are two focused ion beam (FIB) systems, one using gallium and the other xenon ions, and a cleanroom for complementary processing. The choice of which beam

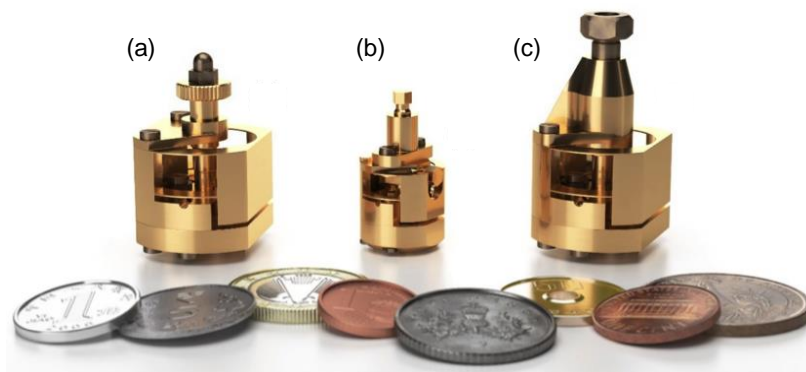


Fig.-4: (a) A compact capacitive dilatometer, developed in the PQM department. (b) An ultra-compact version. (c) A version modified to apply strong uniaxial stress.

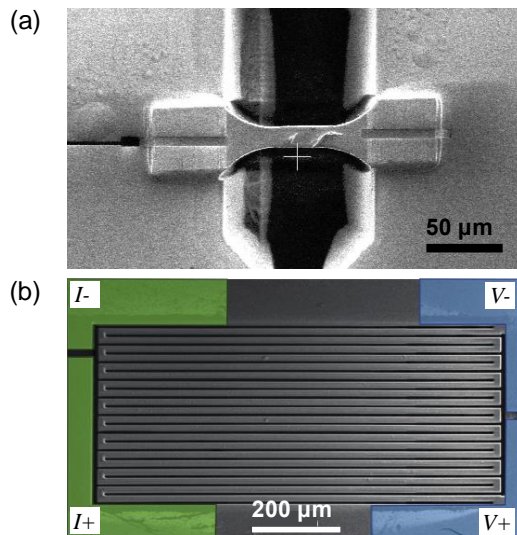


Fig.-5: Examples of microstructuring with focused ion beams. (a) A sample of  $\text{PrV}_2\text{Al}_{20}$  prepared for application of uniaxial stress. (b) A crystal of  $\text{YbRh}_2\text{Si}_2$  with a length-to-width aspect ratio of 1000, for high-resolution measurement of resistivity.

to use depends on the requirements of the intended experiment: the gallium beam offers higher spatial resolution, allowing for feature sizes well below one micron, while the xenon beam offers faster milling at lower spatial resolution.

One generic advantage of ion beam processing is simply the capability to work with very small samples. This is particularly relevant for materials for which high-quality single crystals are not available in sizes that allow conventional experimental approaches. For example, we show in Fig. 5(a) a sample of  $\text{PrV}_2\text{Al}_{20}$  that has been shaped by FIB patterning for uniaxial stress experiments. High-quality single crystals of this material are at present unavailable in sizes larger than  $\sim 0.5$  mm.

With some imagination, qualitatively different experiments are possible. One example is high-precision measurement of the resistivity of high-conductivity compounds. To measure a low resistivity, the sample should generally be prepared with a high length-to-width ratio, in order to increase the resistance and obtain a larger signal. Using FIB patterning, this process can be taken far: an extreme example, of a single crystal of  $\text{YbRh}_2\text{Si}_2$  prepared to have a length-to-width ratio of  $\sim 1000$ , is shown in Fig. 5(b). The purpose was to measure resistivity at  $T \sim 1$  mK [9]. At such low temperatures, the excitation current must be very low to avoid heating at the contacts, so instead an extreme aspect ratio is used to obtain a measurable signal.

Another class of experiments is to study samples of sizes comparable to intrinsic length scales. For example, crystals of  $\text{PdCoO}_2$  and  $\text{PtCoO}_2$  can be grown with low-temperature mean free paths of  $\sim 10$   $\mu\text{m}$ . By studying transport in samples reduced to this size, signatures of ballistic and hydrodynamic electron flow can be observed [10].

More complicated structures are also possible. For example, for heat capacity measurements on microscopic samples, the heater can be made from the sample itself: a meander can be carved from part of the sample, and because it is a part of the same single crystal as the rest of the sample, heat transfer is efficient.

### External Cooperation Partners

H. H. Klauß (Technische Universität Dresden, Germany); M. Le Tacon (Karlsruhe Institute of Technology, Germany); B. Keimer (MPI-FKF, Stuttgart, Germany); K. Moler (Stanford University, USA); S. Nakatsuji (Institute for Solid State Physics, Chiba, Japan); T. Shibauchi (U. of Tokyo, Japan); Y. Maeno (Kyoto U., Japan); S. Brown (U.C. Los Angeles, USA); K. Behnia (Ecole Supérieure de Physique et de Chimie Industrielles, Paris, France); P. Gegenwart (U. of Augsburg, Germany); B. Fauqué (Ecole Supérieure de Physique et de Chimie Industrielles, Paris, France); S. Wiedmann (U. of Bristol, United Kingdom); N. E. Hussey (Nijmegen High Field Magnet Laboratory, Netherlands)

### References

- [1]\* *Strong peak in  $T_c$  of  $\text{Sr}_2\text{RuO}_4$  under uniaxial pressure*, A. Steppke, L. Zhao, M. E. Barber, T. Scaffidi, F. Jerzembeck, H. Rosner, A. S. Gibbs, Y. Maeno, S. H. Simon, A. P. Mackenzie and C. W. Hicks, *Science* **355** (2017) eaaf9398.
- [2]\* *Uniaxial pressure control of competing orders in a high-temperature superconductor*, H. H. Kim, S. M. Souliou, M. E. Barber, E. Lefrancois, M. Minola, M. Tortora, R. Heid, N. Nandi, R. Borzi, G. Garbarino, A. Bosak, J. Porras, T. Loew, M. König, P. M. Moll, B. Keimer, C. W. Hicks and M. Le Tacon, *in preparation*.
- [3] [www.razorbillinstruments.com](http://www.razorbillinstruments.com), 20.08.2018.
- [4]\* *A compact and miniaturized high resolution capacitance dilatometer for measuring thermal expansion and magnetostriction*, R. KÜchler, T. Bauer, M. Brando and F. Steglich, *Rev. Sci. Instrum.* **83** (2012) 095102;  
*A uniaxial stress capacitive dilatometer for high-resolution thermal expansion and magnetostriction under multiextreme conditions*, R. KÜchler, C. Stingl and P. Gegenwart, *Rev. Sci. Instrum.* **87** (2016) 073903.  
*The world's smallest capacitive dilatometer, for high-resolution thermal expansion and magnetostriction in high magnetic fields*, R. KÜchler, A. Wörl, P. Gegenwart, M. Berben, B. Bryant and S. Wiedmann, *Rev. Sci. Instrum.* **88** (2017) 083903.

## PHYSICS OF QUANTUM MATERIALS

- [5] [www.dilatometer.info](http://www.dilatometer.info), 20.08.2018.
- [6]\* *Thermodynamic signatures of the field-induced states of graphite*, D. LeBoeuf, C. W. Rischau, G. Seyfarth, R. K uchler, M. Berben, S. Wiedmann, W. Tabis, M. Frachet, K. Behnia and B. Fauqu e, *Nature Commun.* **8** (2017) 13337.
- [7]\* *Uniaxial-stress tuned large magnetic-shape-memory effect in Ni-Co-Mn-Sb Heusler alloys*, C. Salazar Mejia, R. K uchler, A. K. Nayak, C. Felser and M. Nicklas, *Appl. Phys. Lett.* **110** (2017) 071901.
- [8]\* *Uniaxial stress tuning of geometrical frustration in a Kondo lattice*, R. K uchler, C. Stingl, Y. Tokiwa, M. S. Kim, T. Takabatake, and P. Gegenwart, *Phys. Rev. B* **96** (2017) 241110(R).
- [9]\* *Emergence of superconductivity in the canonical heavy-electron metal YbRh<sub>2</sub>Si<sub>2</sub>*, E. Schuberth, M. Tippmann, L. Steinke, S. Lausberg, A. Steppke, M. Brando, C. Krellner, C. Geibel, R. Yu, Q. Si and F. Steglich, *Science* **351** (2016) 485-488.
- [10]\* *Evidence for hydrodynamic electron flow in PdCoO<sub>2</sub>*, P. J. W. Moll, P. Kushwaha, N. Nandi, B. Schmidt, A. P. Mackenzie, *Science* **351** (2016) 1061-1064.

---

# Clifford.Hicks@cpfs.mpg.de